ApJ in press
Preprint typeset using LaTeX style emulateapj v. 08/17/12

EVIDENCE FOR THE TIDAL DESTRUCTION OF HOT JUPITERS BY SUBGIANT STARS

Kevin C. Schlaufman[1] and Joshua N. Winn[2]
Kavli Institute for Astrophysics and Space Research, Massachusetts Institute of Technology, Cambridge, Massachusetts 02139, USA
Received 2013 March 8; accepted 2013 May 31

ABSTRACT

Tidal transfer of angular momentum is expected to cause hot Jupiters to spiral into their host stars. Although the timescale for orbital decay is very uncertain, it should be faster for systems with larger and more evolved stars. Indeed, it is well established that hot Jupiters are found less frequently around subgiant stars than around main-sequence stars. However, the interpretation of this finding has been ambiguous, because the subgiants are also thought to be more massive than the F- and G-type stars that dominate the main-sequence sample. Consequently it has been unclear whether the absence of hot Jupiters is due to tidal destruction, or inhibited formation of those planets around massive stars. Here we show that the Galactic space motions of the planet-hosting subgiant stars demand that on average they be similar in mass to the planet-hosting main-sequence F- and G-type stars. Therefore the two samples are likely to differ only in age, and provide a glimpse of the same exoplanet population both before and after tidal evolution. As a result, the lack of hot Jupiters orbiting subgiants is clear evidence for their tidal destruction. Questions remain, though, about the interpretation of other reported differences between the planet populations around subgiants and main-sequence stars, such as their period and eccentricity distributions and overall occurrence rates.

Keywords: Galaxy: kinematics and dynamics — planet-star interactions — planets and satellites: detection — stars: evolution — stars: kinematics and dynamics — stars: statistics

1. INTRODUCTION

Although radial velocity planet surveys have mainly targeted main-sequence FGKM stars, there have also been numerous discoveries of Jupiter-mass giant planets around evolved stars. These include moderately evolved subgiant stars, as well as very evolved giant stars.[3] This work has provided evidence that the giant planet population around evolved stars differs from the population orbiting solar-type main-sequence stars, in at least three respects. First, there are fewer close-in giant planets ("hot Jupiters") around evolved stars than main-sequence stars (e.g., Bowler et al. 2010; Johnson et al. 2010a). Second, the orbital eccentricities of long-period giant planets are typically lower when the host star is evolved. Third, a larger fraction of evolved stars appear to host long-period giant planets, although this comparison is more complicated because of the possibility of systematic metallicity differences between the samples of evolved stars and main-sequence stars (e.g., Johnson et al. 2010b).

The work described here was motivated by the desire to understand the first finding, the scarcity of hot Jupiters around evolved stars. Two conflicting interpretations have been proposed. The first possibility is that tidal evolution has destroyed the hot Jupiters that once orbited the evolved stars (e.g., Rasio et al. 1996; Villaver & Livio 2009; Kunitomo et al. 2011; Adamów et al. 2012). The second possibility is that the evolved stars are on average more massive than the main-sequence stars, and the differences in the planet populations are linked to the enhanced stellar mass (e.g., Burkert & Ida 2007; Kretke et al. 2009; Currie 2009). In this picture, hot Jupiters may occur less commonly around massive stars due to differences in (for example) the structure of the protoplanetary disk, or the disk dissipation timescale.

The latter scenario, attributing the differences to stellar mass, is generally favored in the literature. It is supported by the results of fitting stellar-evolutionary models to the observable properties of the evolved stars (their luminosities, surface gravities, and effective temperatures), which confirm that the evolved stars are relatively massive. Johnson et al. (2007) referred to their sample of evolved stars as "retired A stars," because the evolutionary models assign these stars the same masses as main-sequence A5–A9 stars (2.0–1.6 $M_{\odot}$). Recently, though, the fidelity of those evolutionary models was called into question by Lloyd (2011). He argued that the selection criteria that were used to define samples of evolved stars should have resulted in a sample dominated by lower-mass stars, with F- and G-type progenitors rather than A-type. The debate over this claim continues (Johnson et al. 2013). In the meantime, it would be helpful to have a model-independent method for comparing the masses of the evolved stars and the main-sequence stars that have been included in radial velocity surveys.

The observed Galactic space motions (kinematics) of the stars can provide such a comparison. All of the stars under discussion are members of the thin disk of the

kschlauf@mit.edu, jwinn@mit.edu
[1] Kavli Fellow
[2] Physics Department, Massachusetts Institute of Technology, Cambridge, Massachusetts 02139, USA
[3] For subgiant stars, see for example Hatzes et al. (2003), Johnson et al. (2007), Robinson et al. (2007), Fischer et al. (2007), Johnson et al. (2008), Bowler et al. (2010), Johnson et al. (2010a,c), and Johnson et al. (2011a,b). For giant stars, see for example Hatzes & Cochran (1993), Frink et al. (2002), Sato et al. (2003), Setiawan et al. (2005), Butler et al. (2006), Hatzes et al. (2006), Döllinger et al. (2007), Sato et al. (2007), Liu et al. (2008), Sato et al. (2008), Döllinger et al. (2009), Liu et al. (2009), Han et al. (2010), Sato et al. (2010), Lee et al. (2011, 2013), and Omiya et al. (2012).

Milky Way, and empirically it is known that the velocity dispersion of a thin-disk population increases with age (e.g., Binney et al. 2000). This is understood as follows. Thin disk stars form from dense, turbulent gas in the Galactic plane. Because that process is highly dissipative, stellar populations are formed with a very cold velocity distribution. Over time, the velocity distribution is heated due to interactions between the stars and molecular clouds (e.g., Spitzer & Schwarzschild 1951) and transient spiral waves (e.g., Barbanis & Woltjer 1967). Massive stars spend only a short time on the main sequence, and there is very little time for collisions to kinematically heat a population of massive stars. On the other hand, solar-mass stars spend a long time on the main sequence, leaving plenty of time for collisions to kinematically heat a population of solar-mass stars. One would therefore expect a main-sequence thin-disk stellar population's space velocity dispersion to decrease with increasing stellar mass. The same is true even for evolved stars, because a star spends such a small fraction of its life as a subgiant or giant relative to its main-sequence lifetime.

In this paper, we investigate the Galactic velocity dispersion of the population of evolved planet-hosting stars. The kinematic evidence shows that these stars are similar in mass to F5–G5 main-sequence stars. Consequently, the lack of host Jupiters around evolved stars cannot be attributed to mass. The most plausible explanation is that the hot Jupiters have been destroyed, after losing orbital angular momentum to their host stars. We describe our sample of planet-hosting stars in Section 2, we detail our analysis procedures in Section 3, we outline scaling relations for tidal evolution timescales in Section 4, we discuss the results and implications in Section 5, and we summarize our findings in Section 6.

2. SAMPLE DEFINITION

We first extract a list of exoplanet host stars identified with the Doppler technique, using the online database `exoplanets.org` (Wright et al. 2011). We cross-match those stars with the Hipparcos catalog (van Leeuwen 2007) to obtain parallaxes and $B-V$ colors, and with the Tycho-2 catalog (Høg et al. 2000) to obtain apparent V-band magnitudes. We transform the Tycho-2 B_T and V_T magnitudes into approximate Johnson-Cousins V-band magnitudes using the relation $V = V_T - 0.090\,(B_T - V_T)$. Photometry for some of the brightest planet-hosting stars is missing from the Høg et al. (2000) catalog. For those cases we use the original Tycho photometry given by Perryman & ESA (1997). We remove from the list all planet-hosting stars with imprecise parallaxes (fractional uncertainty exceeding 20%). We also obtain the nominal parameters of the host stars and their planets from `exoplanets.org`.

We then define three samples of the planet-hosting stars. The sample of subgiants is defined as those stars with $0.85 < (B-V) < 1.1$ and $1.6 < M_V < 3.1$. The sample of giants consists of stars with $M_V < 1.6$. Finally, a sample of main-sequence F5–G5 planet-hosting stars is defined by the criteria $0.44 < (B-V) < 0.68$ and $3.5 < M_V < 5.1$, taken from Binney & Merrifield (1998). We will show later, based on kinematic evidence, that the typical mass of stars in the main-sequence F5–G5 sample is similar to the typical mass of the stars in the subgiant and giant star samples.[4] Figure 1 is a Hertzsprung-Russell (HR) diagram of planet-hosting stars identified with the radial velocity technique, with our three subsamples highlighted.

Our samples are defined according to observable criteria in color and absolute magnitude, as opposed to model-dependent stellar masses (i.e., masses determined by comparing the observable properties with the outputs of theoretical stellar-evolutionary models). This is because the planet surveyors often define samples according to color and absolute magnitude, and because of the questionable reliability of the model-dependent stellar masses for the subgiants (Lloyd 2011). Nevertheless, one may wonder about the model-dependent masses that have been determined for the stars in our samples. For the subgiants, the model-dependent masses reported in the literature are in the range 0.92–2.0 $M_\odot$, with all but six stars having $M_* > 1.4\ M_\odot$.[5] The giant stars have model-dependent masses reported to be in the range 0.92–2.7 $M_\odot$, with all but 6 stars having $M_* > 1.4\ M_\odot$. The reported model-dependent masses of the main-sequence F5–G5 stars are in the range 0.8–1.4 $M_\odot$.

We also define two samples of main-sequence stars in the solar neighborhood (not necessarily planet-hosting stars) using the Hipparcos catalog, requiring as before that the parallax uncertainty be smaller than 20%. The first sample consists of main-sequence stars with $0.15 < (B-V) < 0.30$ and $1.9 < M_V < 2.7$, corresponding to A5–F0 stars (2–1.5 $M_\odot$) according to Binney & Merrifield (1998). Our intention with this sample is to provide a control sample that will allow a test of the hypothesis that the population of subgiant planet hosts is dominated by "retired A stars". The second sample consists of main-sequence stars with $0.44 < (B-V) < 0.68$ and $3.5 < M_V < 5.1$, corresponding to F5–G5 stars (1.3–0.9 $M_\odot$) according to Binney & Merrifield (1998).

We compute Galactic UVW velocities for all stars for which the systemic radial velocities are available in the catalogs of Gontcharov (2006), Massarotti et al. (2008), or Chubak et al. (2012). In addition to radial velocities, as inputs we use Hipparcos astrometry, parallaxes, and proper motions (van Leeuwen 2007). Enough information is available to compute UVW velocities for all 35 subgiants, 23 of 24 giant stars, and 88 of 91 main-sequence F5–G5 stars. We use the algorithm given in `gal_uvw.pro` available from The IDL Astronomy User's Library. We follow the convention that U is positive towards the Galactic center, V is positive in the direction of Galactic rotation, and W is positive towards the North Galactic pole. We do not correct for motion of the Sun relative to the local standard of rest. For those interested in replicating the results, a comparable data set is publicly available from E. Mamajek[6].

[4] We also constructed samples corresponding to F0–F5, F5–G0, and G0–G5 stars. We settled on F5–G5 for the analysis presented here, because this sample gave the best match to the kinematics of the subgiant planet hosts; see Section 3.1.

[5] If we remove the six stars with model-dependent masses smaller than 1.4 $M_\odot$ from this sample, none of the subsequent analyses are substantially affected.

[6] www.pas.rochester.edu/~emamajek/HIP2008_UVW_SpT_Mv.dat

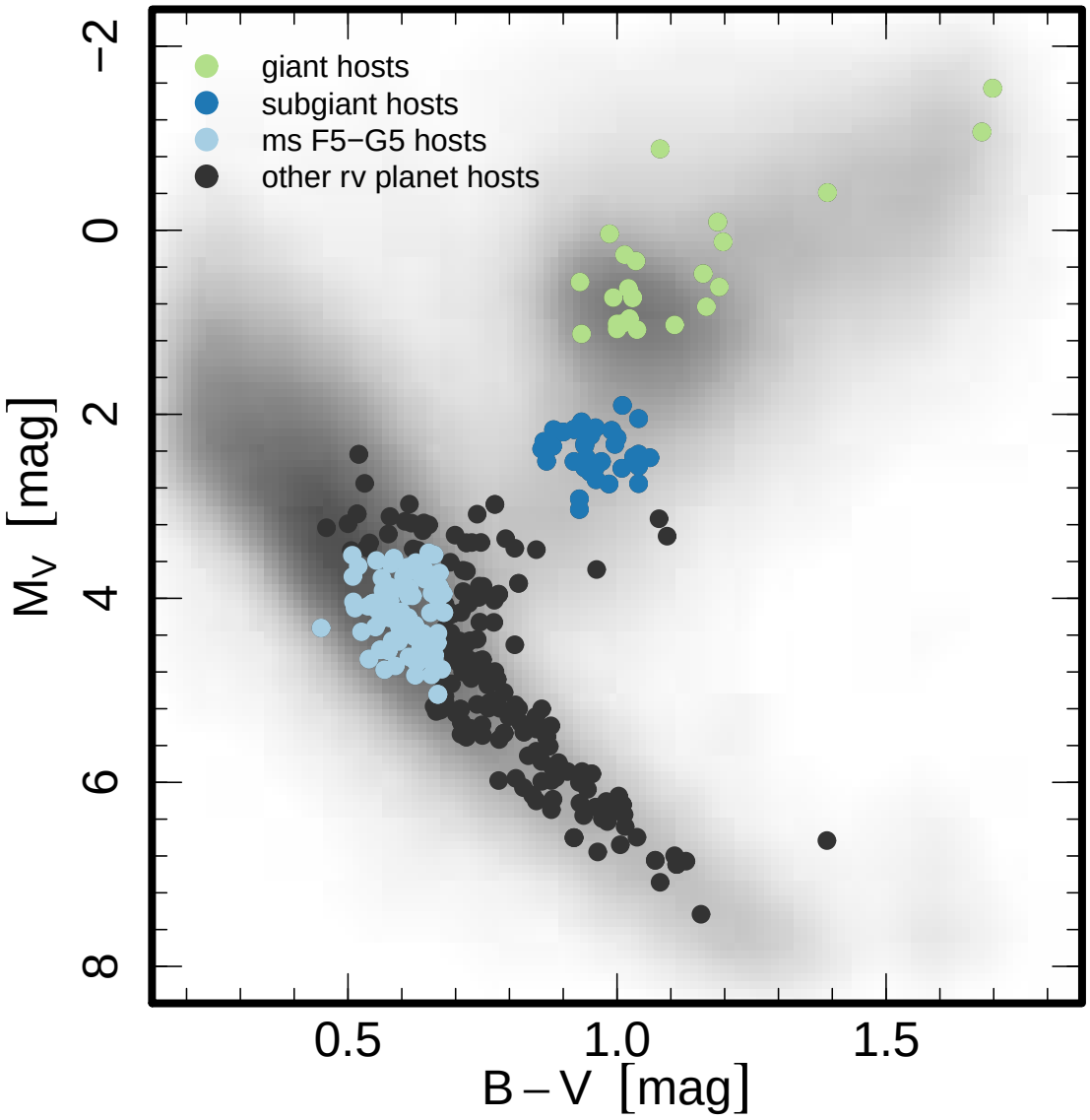

Figure 1. Hertzsprung-Russell diagram of exoplanet host stars identified with the radial-velocity technique listed at `exoplanets.org` (Wright et al. 2011). We isolate and plot three subsamples of the full exoplanet host population: F5–G5 main-sequence stars (light blue points), subgiant stars (dark blue points), and giant stars (green points). We plot all other exoplanet host stars as black points. We plot only those stars that have Hipparcos parallaxes with an uncertainty smaller than 20%. The background shading indicates the density of stars in the entire Hipparcos catalog with relative parallax uncertainties smaller than 20%. The $B-V$ colors come from van Leeuwen (2007) and the V-band photometry is derived from Tycho-2 magnitudes given in Høg et al. (2000) according to the relation $V = V_T - 0.090\,(B_T - V_T)$. Following Binney & Merrifield (1998), we define the F5–G5 sample as those stars with $0.44 < (B-V) < 0.68$ and $3.5 < M_V < 5.1$. We define the subgiant sample as those stars with $0.85 < (B-V) < 1.1$ and $1.6 < M_V < 3.1$. We define the giant sample as those stars with $M_V < 1.6$.

3. SAMPLE COMPARISONS

3.1. *Kinematics*

Figure 2 compares the UVW velocities of the subgiant planet-hosting stars, the solar-neighborhood A5–F0 stars, and the solar-neighborhood F5–G5 stars. As expected, the F5–G5 stars have a much larger velocity dispersion than the A5–F0 stars; they are kinematically hotter. The subgiant planet-hosting stars are also seen to be kinematically hotter than the main-sequence A5–F0 stars, with many stars outside of the 95% ellipse defined by the A5–F0 population. On the other hand, the velocity dispersion of the subgiant planet-hosting stars is comparable to the velocity dispersion of the main-sequence F5–G5 sample.

We quantify the significance of these observations in the following way. First, we calculate the mean UVW velocities of the solar neighborhood main-sequence A5–F0 and F5–G5 samples. We denote these mean velocities by $\bar{U}$, $\bar{V}$, and $\bar{W}$. We then compute

$$\delta_i = \left[\left(U_i - \bar{U}\right)^2 + \left(V_i - \bar{V}\right)^2 + \left(W_i - \bar{W}\right)^2 \right]^{1/2} \quad (1)$$

where U_i, V_i, and W_i are the individual UVW velocity coordinates of a single star. We calculate δ for each star in the subgiant sample and δ' for each star in the so-

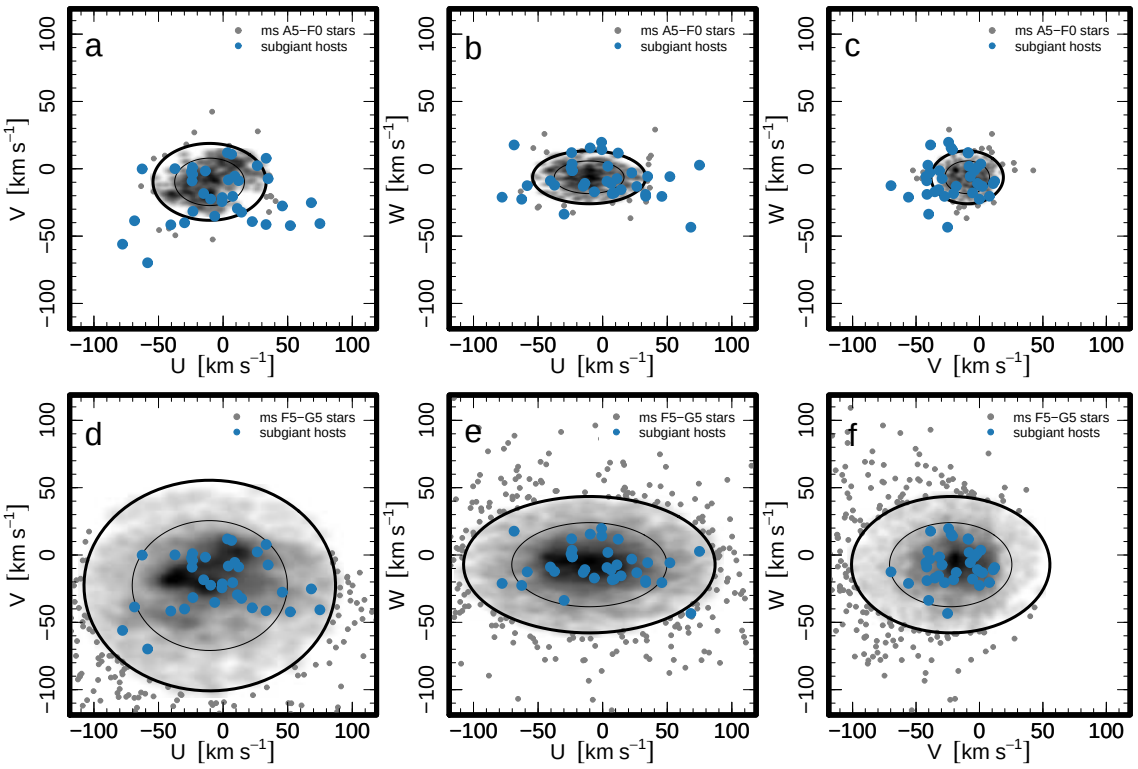

Figure 2. Galactic UVW kinematics of subgiant stars that host exoplanets discovered with the radial-velocity technique. In each panel, we plot the UVW space motions of the subgiant sample as blue points and the density of points in a control sample selected from the Hipparcos catalog as the background shading. We plot outliers in the control sample as gray points. In panels a, b, and c the control sample consists of main-sequence A5–F0 Hipparcos stars with $0.15 < (B-V) < 0.30$ and $1.9 < M_V < 2.7$ (e.g., Binney & Merrifield 1998). In panels d, e, and f the control sample consists of main-sequence Hipparcos F5–G5 stars with $0.44 < (B-V) < 0.68$ and $3.5 < M_V < 5.1$ (e.g., Binney & Merrifield 1998). In each panel, the light (heavy) ellipse is the 68% (95%) velocity ellipsoid of the control sample in that panel. The UVW velocity distribution of the subgiant sample is kinematically much hotter than the UVW velocity distribution of the main-sequence A5–F0 sample. However, it is well matched by the UVW velocity distribution of the main sequence F5–G5 stars. We quantify these observations in Section 3.1. The velocity dispersion of a thin disk stellar population increases with age (e.g., Binney et al. 2000). Since the post–main-sequence phase of stellar evolution is much shorter than the main-sequence phase, the velocity dispersion of a post–main-sequence stellar population depends on the main-sequence lifetimes of its constituent stars. As a result, the large velocity dispersion of subgiant exoplanet host sample relative to the main-sequence A5–F0 population indicates that subgiants spent more time on the main sequence than the A5–F0 stars. Therefore the subgiants are on average lower in mass than the A5–F0 sample, and likely to be similar in mass to the F5–G5 sample.

lar neighborhood A5–F0 sample. We use the Anderson-Darling test (see, e.g., Hou et al. 2009) to compare the sample of subgiant δ_i values to the sample of A5–F0 δ'_i values. We find the probability that the subgiant planet-hosting stars are drawn from the same parent distribution as solar-neighborhood A5–F0 stars to be less than 10^{-6}. Then we repeat the same calculation after computing δ' for each star in the solar neighborhood F5–G5 sample. The result is that there is no reason to reject the hypothesis that the subgiant planet hosts and the F5–G5 stars are drawn from the same population (Anderson-Darling p-value = 0.48).

The UVW space motions of the subgiant planet-hosting stars are incompatible with the hypothesis of recent evolution from a population of A5–F0 main-sequence stars. Their larger velocity dispersion requires that they experienced longer main-sequence lifetimes than the stars in the solar-neighborhood main-sequence A5–F0 sample. This in turn implies that the subgiant planet-hosting stars are less massive than the main-sequence A5–F0 stars. The agreement between the velocity dispersions of the subgiants and the solar-neighborhood main-sequence F5–G5 sample indicates that these two samples likely have similar stellar masses.[7]

This is at odds with the model-dependent masses for the subgiants, which are generally reported to be larger than than the masses of main-sequence F5–G5 stars. While our sample-based test cannot be used to establish the mass of any particular star, we note that there is only a very weak negative correlation (≈ -0.1) between δ and the model-dependent mass. This correlation is not significantly different from zero given the sample size ($N = 35$). The correlation would have needed to be 0.3 or larger in absolute value to have established a genuine correlation at the $p = 0.05$ level.

Figure 3 compares the UVW velocities of the giant planet-hosting stars with the solar-neighborhood main-sequence stars. The UVW velocity dispersion of the giants is also inconsistent with solar-neighborhood main-sequence A5–F0 sample (Anderson-Darling $p < 10^{-6}$). And just as with the subgiants, their velocity dispersion

[7] When we use a control sample of F0–F5 stars rather than F5–G5 stars, the Anderson-Darling test indicates that the F0–F5 sample and the subgiant planet host sample have a probability $p = 0.00033$ of being drawn from the same parent distribution. Thus the typical mass of the subgiant planet hosts is also likely to be smaller than that of the F0–F5 stars.

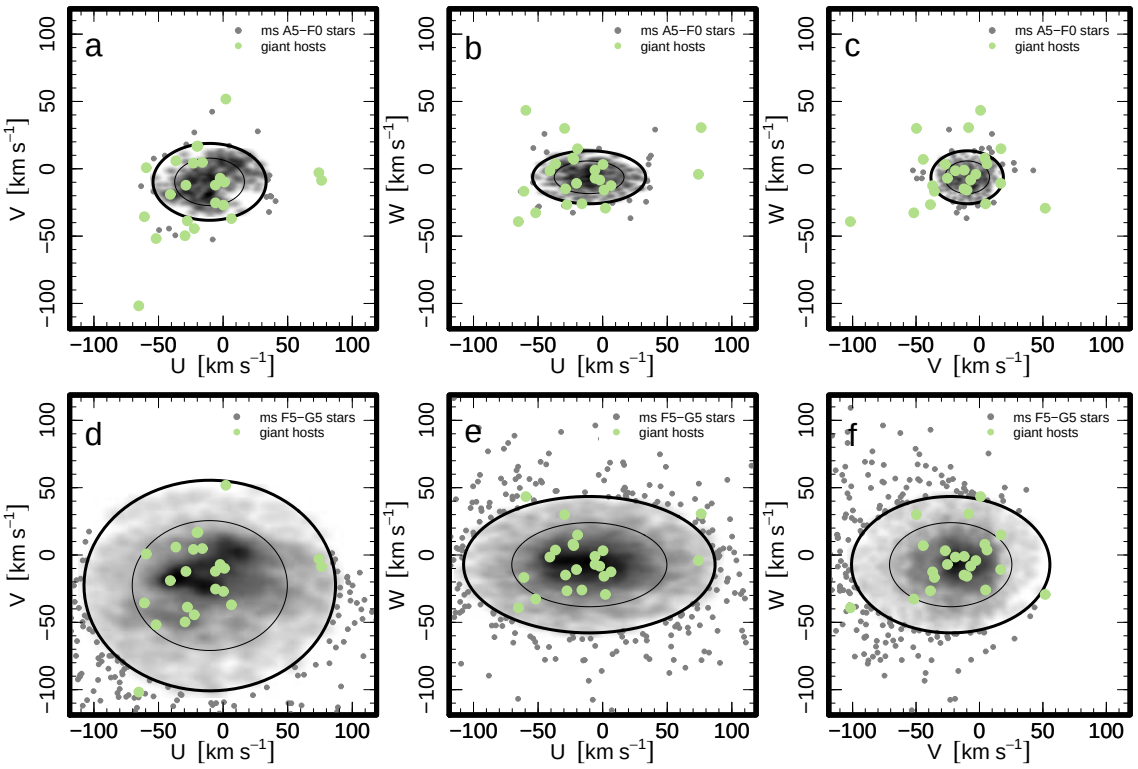

Figure 3. Galactic UVW kinematics of giant stars that host exoplanets discovered with the radial-velocity technique. In each panel, we plot the UVW space motions of the giant sample as green points and the density of points in a control sample selected from the Hipparcos catalog as the background shading. We plot outliers in the control sample as gray points. In panels a, b, and c the control sample consists of main-sequence A5–F0 Hipparcos stars with $0.15 < (B-V) < 0.30$ and $1.9 < M_V < 2.7$ (e.g., Binney & Merrifield 1998). In panels d, e, and f the control sample consists of main-sequence Hipparcos F5–G5 stars with $0.44 < (B-V) < 0.68$ and $3.5 < M_V < 5.1$ (e.g., Binney & Merrifield 1998). In each panel, the light (heavy) ellipse is the 68% (95%) velocity ellipsoid of the control sample in that panel. The UVW velocity distribution of the giant sample is kinematically much hotter than the UVW velocity distribution of the main-sequence A5–F0 sample. However, it is well matched by the UVW velocity distribution of the main-sequence F5–G5 stars. We quantify these observation in Section 3.1. As a result, the typical mass of a star in the giant population is more likely to be similar in mass to a F5–G5 star than an A5–F0 star.

is indistinguishable from the solar-neighborhood main-sequence F5–G5 sample (Anderson-Darling $p = 0.62$). We conclude that the planet-hosting giant stars, like the subgiants, are on average similar in mass to the main-sequence F5–G5 planet hosts.

One of the planet-hosting giants, β Geminorum (Pollux) happens to have a asteroseismic mass determination placing it firmly in the "retired A star" category, with $M_* = 1.91 \pm 0.09\ M_\odot$ (Hatzes et al. 2012). Reassuringly, we find that this star has a UVW velocity of $(-16, 5, -26)$ km s^{-1}, placing it just outside of the 68% contour of the solar-neighborhood main-sequence A5–F0 sample. Therefore this particular star has a low space velocity as expected, and does not call into question the overall result that the sample of planet-hosting giants is dominated by lower-mass stars.

Figure 4 compares the UVW velocities of the planet-hosting F5–G5 stars, and of the solar-neighborhood samples. As expected, we find that the main-sequence F5–G5 planet-hosting stars are kinematically hotter than the solar-neighborhood A5–F0 stars, and they are kinematically indistinguishable from the solar-neighborhood main-sequence F5–G5 sample.

Figures 2, 3, and 4 indicate that on average the subgiant planet-hosting stars are similar in mass to the main-sequence F5–G5 planet hosts. However it is possible that some fraction of the subgiant planet hosts stars are indeed more massive than the F5–G5 planet hosts. To quantify the maximum fraction of massive stars that could be present in the subgiant sample, we use a Monte Carlo simulation. We create many random mixed control samples composed of both solar neighborhood main-sequence A5–F0 and F5–G5 stars. We vary the fraction of main-sequence A5–F0 stars and then compare the velocity dispersion of the subgiant sample to the resultant mixed control samples. We find that control samples including less than ≈40% main sequence A5–F0 stars are generally consistent with the subgiant sample. Consequently, we expect that no more than 40% of the subgiant planet hosts were once A5–F0 stars.[8] Based on a similar calculation, we also find that no more than 40% of the stars in the giant sample were once A5–F0 stars.

We perform a few additional tests of the claim that the subgiants that were selected for the Doppler planet surveys have a typical mass similar to that of F5–G5 stars. First, we repeated the comparisons after swapping the subgiant planet-hosting sample for the sample of southern sky subgiants from the Pan-Pacific Planet Search presented by Wittenmyer et al. (2011). These are not necessarily planet-hosting stars, but they were selected for Doppler surveillance in a similar fashion as the other subgiant planet hosts. We obtain quantitatively similar

[8] Based on similar tests we also expect that no more than 60% of the subgiant planet hosts were once F0–F5 stars.

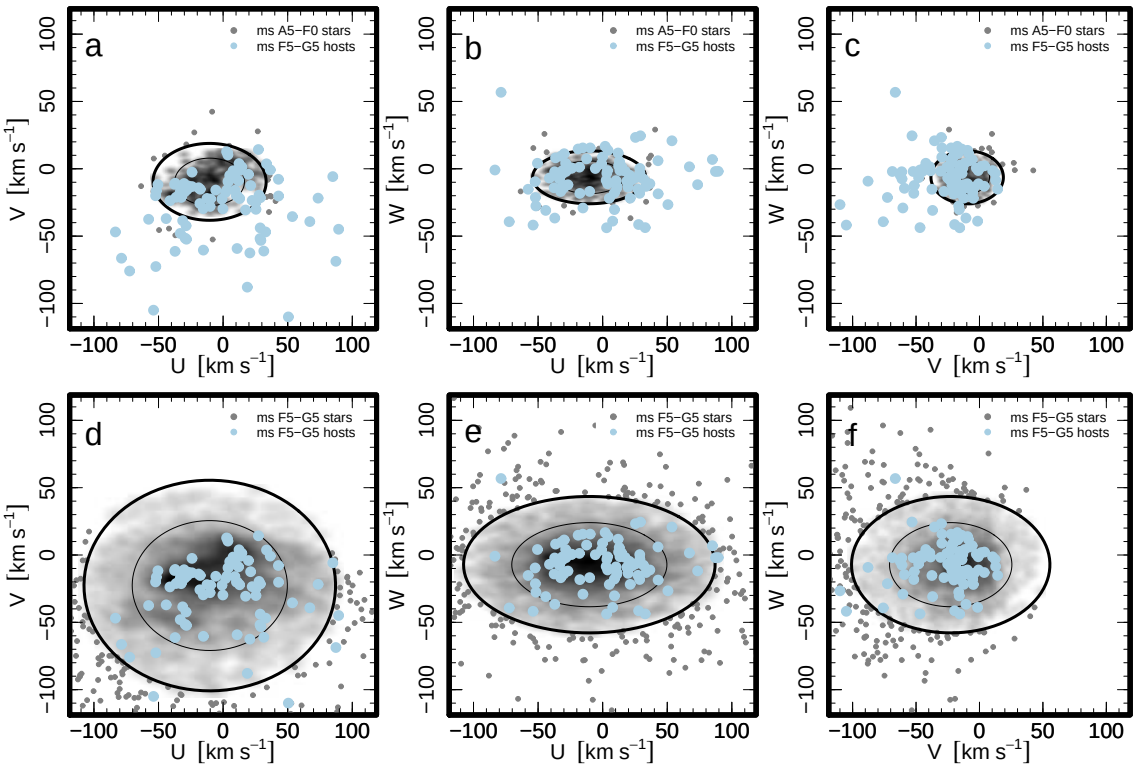

Figure 4. Galactic UVW kinematics of main-sequence F5–G5 stars that host exoplanets discovered with the radial-velocity technique. In each panel, we plot the UVW space motions of the main-sequence F5–G5 sample as light blue points and the density of points in a control sample selected from the Hipparcos catalog as the background shading. We plot outliers in the control sample as gray points. In panels a, b, and c the control sample consists of main-sequence A5–F0 Hipparcos stars with $0.15 < (B-V) < 0.30$ and $1.9 < M_V < 2.7$ (e.g., Binney & Merrifield 1998). In panels d, e, and f the control sample consists of main-sequence Hipparcos F5–G5 stars with $0.44 < (B-V) < 0.68$ and $3.5 < M_V < 5.1$ (e.g., Binney & Merrifield 1998). In each panel, the light (heavy) ellipse is the 68% (95%) velocity ellipsoid of the control sample in that panel. As expected, the UVW velocity distribution of the main-sequence F5–G5 sample is kinematically much hotter than the UVW velocity distribution of the main-sequence A5–F0 sample but well matched by the UVW velocity distribution of the larger Hipparcos main-sequence F5–G5 star sample. We quantify these observations in Section 3.1.

results; the Pan-Pacific search targets are kinematically better matched to F5–G5 stars than to more massive stars. Second, we select subgiant stars from the Hipparcos catalog using the same color and magnitude criteria that we applied to select the planet-hosting subgiant sample. This is intended to mimic the parent population of subgiants from which the planet-hosting stars were identified by the Doppler surveyors. We find that their kinematics are indistinguishable from the kinematics of the planet-hosting subgiants (Anderson-Darling p-value $= 0.30$). We also find the Hipparcos subgiant sample to be kinematically incompatible with an origin in the same parent population as the Hipparcos main sequence A5–F0 sample (Anderson-Darling p-value $< 10^{-6}$). In contrast, the subgiant planet hosts and the main-sequence F5-G5 planet hosts are kinematically consistent with an origin in the same parent population (Anderson-Darling p-value $= 0.5$).

3.2. *Metallicities*

The masses of the subgiant planet-hosting stars are now seen to be similar to those of the main-sequence F5–G5 planet-hosting stars. One may wonder, though, if there are systematic differences in other stellar parameters that may have affected their planet populations. A key parameter is metallicity, which is well known to have a major influence on the properties of giant planets (Santos et al. 2004; Fischer & Valenti 2005). Thus it is important to compare the metallicities of the two samples. Based on the metallicity determinations reported in the literature, we find the average metallicity of the main-sequence sample ([Fe/H] $= 0.05 \pm 0.03$) to overlap with the average metallicity of the subgiant sample ([Fe/H] $= 0.03 \pm 0.03$). Their distributions are consistent with being drawn from the same parent distribution (Anderson-Darling p-value $= 0.3$). Thus at face value the metallicity distributions appear to be equivalent, although in Section 5.3 we discuss the possibility of systematic biases in the reported metallicity values.

3.3. *Orbital Parameters*

The radial velocity surveys are complete for planets with velocity semiamplitude $K > 20$ m s^{-1} and orbital distance $a < 2.5$ AU, corresponding to orbital period $P \lesssim 4$ yr (Johnson et al. 2010b). We therefore focus attention on the population of known planets satisfying these criteria. In Figure 5 we plot the P–e and P–K distributions for the giant planets with $K > 20$ m s^{-1} and $a < 2.5$ AU, for all three samples of planet-hosting stars.

The planets orbiting both samples of evolved stars (subgiants and giants) mainly have periods longer than 100 days. Only one subgiant has a planet with a shorter period, in strong contrast to the main-sequence stars which frequently host short-period planets. Furthermore the planets around the evolved stars are preferentially

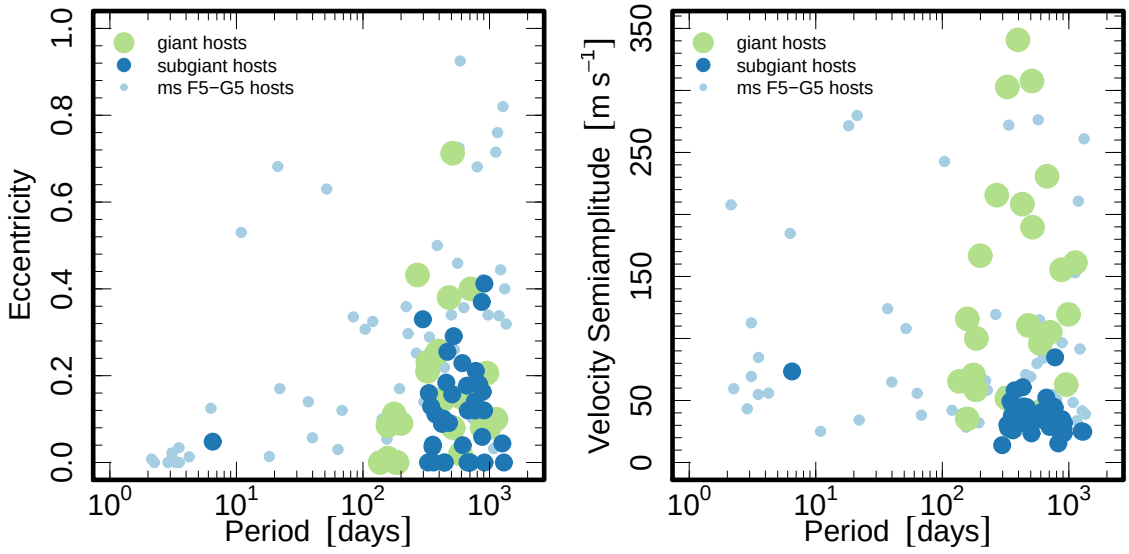

Figure 5. Eccentricities, velocity semiamplitudes (K), and orbital periods for the planets in each of our samples: main-sequence F5–G5 stars (light blue), subgiants (dark blue), and giants (green). For each sample, we only include planets that reside in parts of parameter space in which radial velocity surveys are complete: $K > 20$ m s^{-1} and $a < 2.5$ AU (e.g., Johnson et al. 2010b). There are three significant differences between the samples: (1) there are fewer planets orbiting evolved stars at short periods, (2) the planets around subgiants have lower eccentricities, and (3) the planets around subgiants have smaller K values than those observed around main-sequence stars or giants.

on circular orbits, compared to the more eccentric orbits commonly seen for the planets around main-sequence F5–G5 stars. The mean eccentricities of the planets around subgiants, giants, and main-sequence stars are $\bar{e} = 0.12 \pm 0.02$, $\bar{e} = 0.17 \pm 0.03$, and $\bar{e} = 0.36 \pm 0.04$, respectively. The eccentricity distributions for planets around subgiants, and for planets around giants, are consistent with each other (Anderson-Darling p-value $= 0.3$). However the probability that the eccentricities of the planets around subgiants are drawn from the same parent distribution as the main-sequence sample is less than 10^{-6}. In the next section we will examine the hypothesis that tidal evolution is responsible for these differences in the planet populations.

The right panel of Figure 5 also shows that the planets orbiting subgiants are clustered at low velocity semiamplitudes $K \approx 40$ m s^{-1}, relative to the planets around main-sequence stars. This is despite the fact that planets with larger K values would have been more easily detected. The probability that the K distributions of planets around subgiants and main-sequence stars are drawn from the same parent distribution is less than 10^{-6}.

One finding that is not illustrated in Figure 5 is that the evolved stars are more likely than the main-sequence stars to show evidence for additional longer-period companions, in the form of a long-term radial-velocity trend. At $P > 100$ days, long-term radial-velocity trends occur around 9 of 34 subgiants. In contrast, long-term trends occur in only 2 of 33 main-sequence stars (with giant planets in the complete region of parameter space) and in only 1 out of 24 giant stars. If the distribution of long-term trends were the same for subgiants as for main-sequence stars, the chance of reproducing these numbers would be less than 1 in 40,000.

4. TIDAL TIMESCALES

If the subgiant planet-hosting stars and the main-sequence F5–G5 planet-hosting stars have similar kinematics and metallicities, the differences between their planet populations are not easily attributed to differences in mass or composition. Instead, the observed differences in planet populations are likely to be related to age or stellar radius (which are, of course, correlated). A mechanism for altering planetary systems that is known to depend sensitively on stellar radius is tidal dissipation. Theoretical rates of energy dissipation due to star-planet tidal interactions scale as high powers of the stellar radius ($\propto R_*^5$ in the works cited below). In this section we develop approximate formulas for tidal dissipation rates, to support the discussion in the next section.

Tidal interactions between a star and an orbiting planet allow for the exchange of angular momentum between the bodies while steadily draining energy from the system (Counselman 1973; Hut 1980, 1981). If the star's rotation period is longer than the planet's orbital period, the star spins up and the orbit shrinks. If the total angular momentum of the system exceeds a critical value, the orbit eventually circularizes and the bodies' spins are synchronized and aligned. If however the total angular momentum is too small, then there is no stable equilibrium: the orbit keeps shrinking until the planet is destroyed. It is not yet possible to compute accurate dissipation timescales from first principles. The best that can be done is to establish plausible scaling relationships that are calibrated using observations, as we attempt here.

Eccentricity damping (orbit circularization) can occur either due to dissipation inside of the planet or inside of the star. The timescales for eccentricity damping due to dissipation inside of the planet $t_{e,p}$, due to dissipation inside of the star $t_{e,*}$, and their ratio are (e.g., Mardling 2007; Mazeh 2008)

$$t_{e,p} \approx \frac{2P}{21} \left(\frac{Q_p}{k_p}\right) \left(\frac{M_p}{M_*}\right) \left(\frac{a}{R_p}\right)^5, \quad (2)$$

$$t_{e,*} \approx \frac{2P}{21} \left(\frac{Q_*}{k_*}\right) \left(\frac{M_*}{M_p}\right) \left(\frac{a}{R_*}\right)^5, \quad (3)$$

$$\frac{t_{e,*}}{t_{e,p}} = \left(\frac{Q_*/k_*}{Q_p/k_p}\right)\left(\frac{M_*}{M_p}\right)^2\left(\frac{R_p}{R_*}\right)^5, \quad (4)$$

where P is the orbital period, a is the orbital semimajor axis, Q_p and Q_* are the tidal quality factors of the planet and star, k_p and k_* are their tidal Love numbers, M_p and M_* are their masses, and R_p and R_* are their radii. Assuming constant Q_p, k_p, M_p, R_p, and M_*, the scaling relations for the timescale for orbit circularization due to dissipation inside of the planet and inside of its host star are

$$\frac{t_{e,p,2}}{t_{e,p,1}} = \left(\frac{P_2}{P_1}\right)\left(\frac{a_2}{a_1}\right)^5, \quad (5)$$

$$\frac{t_{e,*,2}}{t_{e,*,1}} = \left(\frac{P_2}{P_1}\right)\left(\frac{Q_{*,2}/k_{*,2}}{Q_{*,1}/k_{*,1}}\right)\left(\frac{R_{*,1}}{R_{*,2}}\right)^5\left(\frac{a_2}{a_1}\right)^5. \quad (6)$$

It is commonly understood that for main-sequence stars with planets, orbital circularization is mainly due to dissipation within the planet. This is because the usual assumptions $Q_*/k_* \sim 10^6$, $Q_p/k_p \sim 10^5$, $M_* = 1\ M_\odot$, $M_p = 1\ M_{\rm Jup}$, $R_* = 1\ R_\odot$, $R_p = 1\ R_{\rm Jup}$ lead to $t_{e,*}/t_{e,p} \sim 100$. We use this fact to provide a rough calibration for the dissipation timescale. Figure 5 shows that planets orbiting main-sequence stars inside of $P = 5$ days are on nearly circular orbits, while planets orbiting outside of $P = 10$ days are frequently on eccentric orbits. The timescale for orbit circularization in the shorter-period systems must be significantly shorter than the ages of the systems. We will therefore assume that the circularization timescale $\tau_{e,p}$ at $P = 5$ days for a solar-mass star with $Q_*/k_* \sim 10^6$ and a planet with the mass and radius of Jupiter and $Q_p/k_p \sim 10^5$ is $\tau_{e,p} = 1$ Gyr.

When the host star is a subgiant with $R_* = 4\ R_\odot$, then $t_{e,*}/t_{e,p} \sim 0.01$ and circularization should be mainly due to dissipation inside of the star (e.g., Rasio et al. 1996). Using Equations (4), (5), and (6) plus the calibration presented above we may write

$$t_{e,*} = \tau_{e,p}\Theta\left(\frac{P}{5\text{ days}}\right)\left(\frac{a}{0.06\text{ AU}}\right)^5, \quad (7)$$

where

$$\Theta \equiv \left(\frac{Q_*/k_*}{Q_p/k_p}\right)\left(\frac{M_*}{M_p}\right)^2\left(\frac{R_p}{R_*}\right)^5. \quad (8)$$

Then, taking the overall eccentricity-damping timescale t_e to be the smaller of the two dissipation timescales (inside the planet or inside the star), we have

$$t_e = \tau_{e,p}\left(\frac{P}{5\text{ days}}\right)\left(\frac{a}{0.06\text{ AU}}\right)^5 \min(1, \Theta). \quad (9)$$

As for tidal evolution of the orbital distance a, the scaling relation is thought to be (e.g., Lin et al. 1996)

$$t_a \propto \frac{M_*^{1/2}(Q_*/k_*)a^{13/2}}{M_p R_*^5}. \quad (10)$$

Figure 5 shows that there are many planets orbiting main sequence stars at $P \approx 5$ days, but few at $P \approx 1$ day. Assuming this difference to reflect the tidal decay of the shortest-period orbits leads to a rough calibration of the tidal decay timescales. If we assume that the timescale for orbital drift τ_a of a 1 $M_{\rm Jup}$ planet orbiting at $P = 5$ days a $Q_*/k_* \sim 10^6$, 1 $M_\odot$, and 1 $R_\odot$ host star is $\tau_a = 10$ Gyr, then we have

$$t_a = \tau_a\left(\frac{Q_*/k_*}{10^6}\right)\left(\frac{R_*}{R_\odot}\right)^{-5}\left(\frac{a}{0.06\text{ AU}}\right)^{13/2}. \quad (11)$$

Equations (9) and (11) were used to calculate t_e and t_a as a function of orbital period and stellar radius, for a fiducial solar-mass star with a Jovian planet. The results are shown in Figure 6, which also displays the periods and stellar radii of the various samples of exoplanet systems considered in this paper. The stellar radii are based on the empirical calibration given by Torres et al. (2010).

There are two other criteria that must be satisfied for tidal decay. First, since tides only cause orbital decay if the stellar rotation period is longer than the orbital period, we indicate in Figure 6 the maximum stellar rotation period that would be expected for stars in the different samples. These are based on the observed projected rotation rates ($v \sin i$) and estimated radii of the planet host stars, using

$$P_{\rm rot} \lesssim \tfrac{2\pi R_*}{v \sin i}. \quad (12)$$

The upper limit on $P_{\rm rot}$ was computed for each star. Then, the median of these upper limits was computed for each sample, and plotted in the left panel of Figure 6.

Second, the total angular momentum of the system $L_{\rm tot}$ must be lower than the critical value $L_{\rm crit}$ necessary for a stable equilibrium (in which the star and planet have achieved spin–orbit synchronization and alignment). The total angular momentum can be written

$$L_{\rm tot} = L_{\rm orb} + L_{{\rm rot},*} + L_{{\rm rot},p}, \quad (13)$$

$$L_{\rm orb} = \mu\left[GM_{\rm tot}a(1-e^2)\right]^{1/2}, \quad (14)$$

$$L_{{\rm rot},*} = g_*^2 M_* R_*^2 \omega_*, \quad (15)$$

$$L_{{\rm rot},p} = g_p^2 M_* R_p^2 \omega_p, \quad (16)$$

where $\mu = (M_* M_p)/(M_* + M_p)$ is the reduced mass and $M_{\rm tot} = M_* + M_p$ is the total mass of the system. Here $g_*^2 = 0.06$ and $g_p^2 = 0.25$ are the radii of gyration of star and planet, assuming the solar and Jovian values respectively. Likewise, ω_* and ω_p are the angular velocities of star and planet. The rotational angular momentum of the planet is negligible. The value of $L_{\rm crit}$ is (e.g., Hut 1980; Matsumura et al. 2010)

$$L_{\rm crit} = 4\left[\frac{G^2}{27}\frac{M_*^3 M_p^3}{M_* + M_p}(I_* + I_p)\right]^{1/4}, \quad (17)$$

where $I_* = g_*^2 M_* R_*^2$ and $I_p = g_p^2 M_p R_p^2$. Assuming $M_* = 1\ M_\odot$, $M_p = 1\ M_{\rm Jup}$, $R_* = 4\ R_\odot$, and $R_p = 1\ R_{\rm Jup}$ characteristic of an evolved star with a giant planet, then all systems with $a \lesssim 0.35$ AU, or approximately $P \lesssim 75$ days, are tidally unstable. Such planets will ultimately be engulfed, if the host star's rotational angular momentum was initially comparable to the current solar value.

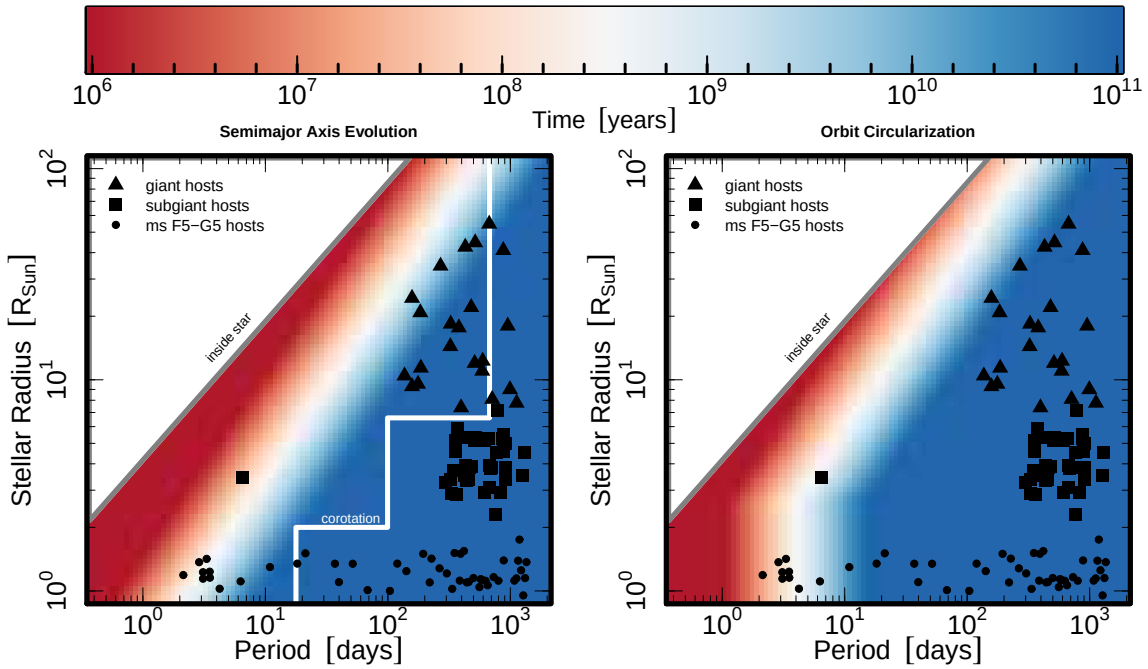

Figure 6. Tidal timescales as a function of period and stellar radius. *Left*: Timescale t_a for semimajor axis evolution (orbital decay) for planets inside the corotation radius (marked approximately by the white line). *Right*: Timescale t_e for orbit circularization. The timescales were computed as described in the text, assuming $M_* = 1\ M_\odot$, $M_p = 1\ M_{\rm Jup}$, $R_p = 1\ R_{\rm Jup}$, $Q_*/k_* = 10^6$, and $Q_p/k_p = 10^5$. For planets to the left of the white diagonal band, the calculated tidal timescale is short compared to the duration over which a solar-mass, solar-metallicity star exists as a subgiant or at the base of the giant branch (e.g., Dotter et al. 2008). The left-hand figure shows that the scarcity of $P < 10$ day planets around subgiants is a seemingly inevitable consequence of tidal decay. The right-hand figure shows that the tendency for planets around subgiants to have nearly circular orbits all the way out to $P \approx 200$ days can only be explained if stars become much more dissipative as they evolve off of the main sequence ($Q_*/k_* \sim 10^2$). Such a scenario would also imply enhanced rates for tidal decay, and could explain the scarcity of planets around subgiants all the way out to $P \approx 100$ days.

5. DISCUSSION

5.1. *Hot Jupiters*

The left panel of Figure 6 shows that there is no difficulty explaining the lack of hot Jupiters around subgiants with periods between 1 and 10 days. Although such planets' orbits may be stable for a Hubble time around a main-sequence stars, once the host star evolves and reaches a radius of 4 $R_\odot$, tidal dissipation rates increase by a factor of $\sim 10^2$. Those same planets would experience orbital decay in a few 100 Myr, comparable to the time that their host stars spend as subgiants (e.g., Dotter et al. 2008). Tidal destruction has already been noted as a theoretical possibility by Villaver & Livio (2009) and Kunitomo et al. (2011), at least for giant stars with $R_* \gtrsim 20\ R_\odot$. It has also been suggested by Lloyd (2011), among others. Now that the subgiants are seen to have similar masses as the main-sequence sample, tidal destruction seems to be the inevitable explanation for the lack of close-in giant planets orbiting subgiants relative to main-sequence stars.

One might wonder if it is possible to find additional supporting evidence for tidal destruction of hot Jupiters based on the observed rotation rates of subgiants, since the accretion of angular momentum from a disrupted giant planet could affect the rotation rate. Suppose a star with mass 1.3 $M_\odot$, radius 1.1 $R_\odot$, radius of gyration $I/MR^2 = 0.06$ (the solar value), and rotation period $P_{\rm rot} = 10$ d accretes a 1 $M_{\rm Jup}$ planet initially orbiting at 0.1 AU, and absorbs all of its orbital angular momentum. The final rotation period of that star when it reaches $R_* = 4\ R_\odot$ would be 24 days. Had it not absorbed its planet's orbital angular momentum, then its rotational period would have been 130 days. This seems like a significant difference. However, the radii of subgiants are generally uncertain by a factor of two or more. If instead the subgiant had a radius of $R_* = 8\ R_\odot$, then its rotation period after absorbing its planet's orbital angular momentum would be 94 days. Consequently, identifying angular momentum enhancement in evolved stars will be difficult without accurate stellar radii.

The accretion of metal-enriched material from a disrupted giant planet could also affect the observed chemical abundances of an evolved star. Indeed, the accretion of solid material was initially considered as one possible explanation for the enhanced metallicity of the solar-type stars identified as giant planet hosts (e.g., Laughlin 2000). Following the calculation by Laughlin (2000), the accretion of a Jupiter-mass planet with $Z \approx 0.1$ into the 0.5 $M_\odot$ convective envelope of an evolved solar metallicity star will only increase the star's observed metallicity by 0.01 dex – an imperceptibly small increase.

5.2. *Intermediate-period Giant Planets*

Although tidal destruction is a natural explanation for the lack of hot Jupiters around subgiants, the relative scarcity of giant planets with periods between 10 and 100 days cannot be explained as the consequence of tidal destruction unless the tidal dissipation rate for subgiants is 3-4 orders of magnitude faster than estimated in the previous section (and plotted in Figure 6). One possibility is that dissipation becomes faster not only because of

an enlarged stellar radius, but also a decrease in Q_*/k_* due to the changing stellar structure. This could also explain the observation that the shortest-period planets seen around subgiants ($P \approx 200$ days) tend to have circular orbits: such planets would be undergoing tidal eccentricity damping due to dissipation within the host star. This is in contrast to the hot Jupiters observed around main-sequence stars, for which dissipation within the planet is likely to be the primary cause of eccentricity damping. Furthermore it would not be surprising for a subgiant to have a lower Q_*/k_* than a main-sequence star. The strength of tidal evolution in evolved stars is thought to depend on the mass of their convective envelopes (Rasio et al. 1996), and the mass in the convective envelope of a solar-type star increases by an order of magnitude as a subgiant between the main sequence turnoff and the base of the red giant branch (Sackmann et al. 1993).

We digress momentarily to point out that Figure 1 reveals that most of the *giant* planet-hosting stars (as opposed to subgiants) are concentrated in the so-called "red clump" — a region of the HR diagram where the red giant branch overlaps with the horizontal branch for a solar-metallicity stellar population. Without asteroseismic observations, we cannot confidently assign individual stars to one or the other of those two populations. Unfortunately this means the giants are less useful than the subgiants in understanding the tidal evolution of planetary systems, for the following reason. The stars on the horizontal branch are currently burning helium in their cores after an initial ascent up the giant branch. They very likely had larger radii at the tip of the red giant branch than they currently possess. Since tidal effects depend strongly on stellar radius, the tidal evolution of any close-in exoplanets depends strongly on the sizes of the giant stars at the tip of the red giant branch — which are unobserved and poorly constrained. The subgiants invite a more straightforward interpretation, since they are presently as large as they have ever been since the planet-formation epoch.

Putting these pieces together, a scenario that explains many of our observations is as follows. Stars become more dissipative as they evolve off of the main sequence, both because the stellar radius increases and also because Q_*/k_* decreases by 3-4 orders of magnitude. Consequently, planets orbiting inside of the corotation radius ($P \lesssim 100$ days) lose angular momentum relatively quickly through tidal interactions. Planets just outside of corotation are pushed out and pile up at $P \approx 200$ days, while also undergoing eccentricity damping. Extending this scenario to the giant stars is also possible. As the host stars continue to move up the red giant branch, they expand and their rotation slows. As a consequence, the corotation radius is enlarged. Those planets that were previously secure at $P \approx 200$ days now find themselves losing orbital angular momentum. These planets are not necessarily destroyed, though, because the host stars' trip up the red giant branch is brief. The orbital distances may shrink only modestly before the host stars start burning helium in their cores, contract, and settle onto the horizontal branch.

5.3. *Occurrence Rates of Giant Planets*

Some of the observed differences between the planet populations around subgiants and main-sequence stars have no obvious interpretation in terms of tidal interactions. First, there is no simple explanation for the higher occurrence rate of long-period giant planets around subgiant stars. According to Bowler et al. (2010), the occurrence rate of giant planets with $a < 3$ AU is $26^{+9}_{-8}\%$ as compared to 5–10% for main-sequence stars. More recently, Johnson et al. (2010b) accounted for the effect of metallicity on planet occurrence and determined that the occurrence rate of giant planets with $a \lesssim 2.5$ AU is $11\pm2\%$ for subgiants, as compared to $6.5\pm0.7\%$ for main-sequence stars. In either case, these offsets represent a 2-3σ difference.

A second and related point is that tides cannot explain the higher incidence of velocity trends noted at the end of Section 3.3. Tides are too weak to affect planets with such long periods that they are observed only as linear trends in a subgiant's radial velocity curve.

Third, and most puzzling, is the clustering of K values between 10–50 m s^{-1} for the subgiants, as compared to the broader distributions 10–300 m s^{-1} for planets in the same period range around both main-sequence stars and giants. The timescale for tidal evolution is proportional to planet mass, raising the possibility that only low-mass planets (small K values) persist once a star evolves off of the main sequence. But any tidal explanation would struggle to explain why the giant stars (which are even more evolved than subgiants) still harbor more massive planets. Future work is needed to understand these three differences.

One possibility is that the average metallicity of the stars in the subgiant sample is higher than that of the main-sequence sample, despite the comparison made in Section 3.2 suggesting that the metallicities are similar. Giant planet occurrence rates are known to be strongly dependent on host star metallicity (e.g., Santos et al. 2004; Fischer & Valenti 2005). In particular Fischer & Valenti (2005) found that the probability of giant planet occurrence P_p scales as

$$P_p \propto 10^{2\left[\mathrm{Fe/H}\right]}. \tag{18}$$

In that case, the increased planet occurrence rate for subgiants reported by Johnson et al. (2010b) could be explained by a residual systematic metallicity offset of $\log(\sqrt{11/6.5}) \approx 0.1$ dex in [Fe/H]. At the 1σ limits of the Johnson et al. (2010b) occurrence rates, even a residual offset as small as $\log(\sqrt{9/7.2}) \approx 0.05$ dex in [Fe/H] could explain the apparently larger occurrence rate of giant planets in the subgiant sample.

Such an offset does not seem out of the question. The metallicities of the subgiants and many FG planet host stars in the control sample have been measured with the Spectroscopy Made Easy package (SME; Valenti & Piskunov 1996) and other similar spectral-fitting codes. The metallicity values returned by SME are known to have systematic biases depending on effective temperature $T_{\rm eff}$ (e.g., Section 6.4 of Valenti & Fischer 2005). Although Valenti & Fischer (2005) attempt to correct for this bias, perhaps there still exists a residual offset of 0.1 dex in [Fe/H] when comparing the main-sequence F5–G5 sample ($T_{\rm eff} \approx 6000$ K) to the subgiant

sample (≈5000 K). Indeed, strong correlations between the values of $T_{\rm eff}$ and [Fe/H] generated by SME were recently identified by Torres et al. (2012), who demonstrated that SME reports cooler temperatures (100 K) and higher metallicities (0.1 dex) than a line-by-line MOOG-like analysis (Sneden 1973). A homogeneous MOOG-like line-by-line stellar parameter analysis of a large sample of both FGK dwarf and subgiant planet-host stars might help to resolve this issue.

We also note that in calculating the dependence of giant planet occurrence rates on stellar mass and metallicity, Johnson et al. (2010b) assumed that the effects of mass and metallicity were separable, even though there is a significant positive correlation between the reported stellar masses and metallicities (see their Figure 2). As we have shown, the subgiant stars are not likely to be especially massive. As a result, some of the increased planet occurrence signal in the subgiant sample was likely misattributed to mass instead of metallicity. For that reason, the metallicity corrections necessary to directly compare the giant planet incidence rate of main-sequence FGK dwarfs and subgiants may have been underestimated by Johnson et al. (2010b).

More speculative is the possibility raised by Lloyd (2011) that some of the radial-velocity signals detected for subgiant stars do not represent planets, but rather stellar oscillations. The oscillations would need to be nonradial to avoid producing large brightness variations in contradiction with the observations. Nonradial oscillations can produce low-amplitude, sinusoidal radial velocity variations (e.g., Hatzes 1996), though usually with smaller amplitudes and shorter periods. To our knowledge nonradial oscillations of subgiants producing signals as large as tens of m s^{-1} with periods of hundreds of days have never been empirically established, nor have they been theoretically predicted. We note, though, that the literature does contain examples of similar quasi-sinusoidal variations that are at least suspected to be the result of nonradial oscillations, in both more evolved and less evolved stars (Hatzes & Cochran 1999; Desort et al. 2009). Perhaps the intense scrutiny of the subgiants by the Doppler surveyors has revealed a new mode of stellar pulsation. In addition to bringing the occurrence rate of giant planets around subgiants into better agreement with the main-sequence stars, this might help to explain the clustering of K values. The physics of the hypothetical pulsations might naturally select a particular range of velocities, whereas the planet-induced velocity amplitudes would depend on three different independent variables (M_p, i, and P) and should combine to produce a wide range of K values.

5.4. *Stellar Mass Loss*

One might also wonder if stellar mass loss contributes to the orbital evolution of planets around subgiant stars, in addition to tidal effects. Mass loss on the red giant branch is frequently parametrized using the Reimers relation (e.g., Kudritzki & Reimers 1978)

$$\frac{dM_*}{dt} = \eta \left(4 \times 10^{-13}\right) \frac{L_*(t) R_*(t)}{M_*} \frac{M_\odot}{\rm yr}, \qquad (19)$$

where L_*, R_*, and M_* are the stellar luminosity, radius, and mass in solar units. The dimensionless parameter η is in the range $0.4 \lesssim \eta \lesssim 0.8$ (e.g., Sackmann et al. 1993) and frequently set to $\eta = 0.5$ (e.g., Kudritzki & Reimers 1978; Hurley et al. 2000). Taking the median luminosity, radius, and isochrone mass of our subgiant planet host sample $L_* = 9.5\ L_\odot$, $R_* = 3.8\ R_\odot$, and $M_* = 1.6\ M_\odot$, the expected mass loss is rate is $dM_*/dt \approx 5 \times 10^{-12}\ M_\odot\ {\rm yr}^{-1}$. Over the 500 Myr a solar-type star spends as a subgiant, the total mass lost is only $M_{\rm loss} \lesssim 0.01\ M_\odot$. Thus, mass loss is unlikely to affect the orbital evolution of close-in giant planets orbiting subgiants or stars at the base of the red giant branch.

6. CONCLUSIONS

Subgiant stars are observed to host fewer close-in giant planets than main-sequence stars, but have a systematically higher giant planet occurrence rate when integrated over all periods. These differences have been attributed to the increased mass of the subgiant planet hosts relative to main-sequence planet hosts. We find that the Galactic kinematics of subgiant stars that host giant planets demand that on average they be similar in mass to solar-type main-sequence planet-hosting stars. Therefore, the best explanation for the lack of hot Jupiters around evolved stars is tidal destruction of the hot Jupiters they once possessed. If tidal dissipation inside their host stars is also responsible for circularizing the orbits of the giant planets orbiting subgiants at $P \approx 200$ days, then tides should also have been strong enough to destroy any giant planets inside of corotation ($P \lesssim 100$ days). Planets outside of corotation may have extracted angular momentum from their host stars and moved to longer orbital periods, explaining the sudden appearance of planets around subgiant stars at $P \approx 200$ days. The apparent 2-3σ increase in the incidence of long-period giant planets around subgiant stars relative to main-sequence stars is difficult to explain. It may be the result of systematic underestimates of the metallicities of subgiant stars or (more speculatively) hitherto unknown modes of stellar pulsation among the subgiants that masquerade as long-period giant planets.

It is also important to note that the kinematic equivalence of the subgiant and main-sequence samples suggests that the theoretical stellar-evolutionary models that were used to infer larger masses for the subgiants need to be re-evaluated. In particular, as suggested by Lloyd (2011) it may be necessary to reassess the applicability of a mixing-length model of convection that is calibrated for the Sun to low surface gravity stars that are not even quasi-stationary and that are developing shells of superadiabatic convection (e.g., Robinson et al. 2004; Cassisi 2012).

There are also potentially important implications of our suggestion that stars become much more dissipative as they evolve off of the main sequence, such that $Q_*/k_* \sim 10^{2-3}$. If this is so, then the Earth will very likely be destroyed as the Sun expands to nearly 100 times its current size near the tip of the red giant branch. Previously it was thought that the orbital evolution of the Earth could not even be predicted qualitatively as it seemed to depend on the details of the Sun's mass loss on the giant branch (e.g., Sackmann et al. 1993; Rasio et al. 1996). Thus the subgiant planet searches may have—quite unexpectedly—clarified the Earth's ultimate fate.

We thank John Johnson, Adam Kraus, Greg Laughlin, Jamie Lloyd, Nevin Weinberg, and the anonymous referee for their comments and constructive criticism. This research has made use of NASA's Astrophysics Data System Bibliographic Services, the Exoplanet Orbit Database and the Exoplanet Data Explorer at exoplanets.org, and both the SIMBAD database and VizieR catalogue access tool, CDS, Strasbourg, France. The original description of the VizieR service was published by Ochsenbein et al. (2000). It has also used The IDL Astronomy User's Library, a service of the Astrophysics Science Division (ASD) at NASA's GSFC. Support for this work was provided by the MIT Kavli Institute for Astrophysics and Space Research through a Kavli Postdoctoral Fellowship.

REFERENCES

Adamów, M., Niedzielski, A., Villaver, E., Nowak, G., & Wolszczan, A. 2012, ApJ, 754, L15
Barbanis, B., & Woltjer, L. 1967, ApJ, 150, 461
Binney, J., Dehnen, W., & Bertelli, G. 2000, MNRAS, 318, 658
Binney, J., & Merrifield, M. 1998, Galactic Astronomy (Princeton, NJ: Princeton Univ. Press)
Bowler, B. P., Johnson, J. A., Marcy, G. W., et al. 2010, ApJ, 709, 396
Burkert, A., & Ida, S. 2007, ApJ, 660, 845
Butler, R. P., Wright, J. T., Marcy, G. W., et al. 2006, ApJ, 646, 505
Cassisi, S. 2012, in Astrophys. Space Sci. Proc. 14, Red Giants as Probes of the Structure and Evolution of the Milky Way, ed. A. Miglio, J. Montalban, & A. Noels (Berlin Heidelberg: Springer-Verlag), 57
Chubak, C., Marcy, G., Fischer, D. A., et al. 2012, arXiv:1207.6212
Counselman, C. C., III 1973, ApJ, 180, 307
Currie, T. 2009, ApJ, 694, L171
Desort, M., Lagrange, A.-M., Galland, F., et al. 2009, A&A, 506, 1469
Döllinger, M. P., Hatzes, A. P., Pasquini, L., Guenther, E. W., & Hartmann, M. 2009, A&A, 505, 1311
Döllinger, M. P., Hatzes, A. P., Pasquini, L., et al. 2007, A&A, 472, 649
Dotter, A., Chaboyer, B., Jevremović, D., et al. 2008, ApJS, 178, 89
Fischer, D. A., & Valenti, J. 2005, ApJ, 622, 1102
Fischer, D. A., Vogt, S. S., Marcy, G. W., et al. 2007, ApJ, 669, 1336
Frink, S., Mitchell, D. S., Quirrenbach, A., et al. 2002, ApJ, 576, 478
Gontcharov, G. A. 2006, Astronomy Letters, 32, 759
Han, I., Lee, B. C., Kim, K. M., et al. 2010, A&A, 509, A24
Hatzes, A. P. 1996, PASP, 108, 839
Hatzes, A. P., & Cochran, W. D. 1993, ApJ, 413, 339
Hatzes, A. P., & Cochran, W. D. 1999, MNRAS, 304, 109
Hatzes, A. P., Cochran, W. D., Endl, M., et al. 2003, ApJ, 599, 1383
Hatzes, A. P., Cochran, W. D., Endl, M., et al. 2006, A&A, 457, 335
Hatzes, A. P., Zechmeister, M., Matthews, J., et al. 2012, A&A, 543, A98
Høg, E., Fabricius, C., Makarov, V. V., et al. 2000, A&A, 355, L27
Hou, A., Parker, L. C., Harris, W. E., & Wilman, D. J. 2009, ApJ, 702, 1199
Hurley, J. R., Pols, O. R., & Tout, C. A. 2000, MNRAS, 315, 543
Hut, P. 1980, A&A, 92, 167
Hut, P. 1981, A&A, 99, 126
Johnson, J. A., Aller, K. M., Howard, A. W., & Crepp, J. R. 2010b, PASP, 122, 905
Johnson, J. A., Bowler, B. P., Howard, A. W., et al. 2010c, ApJ, 721, L153
Johnson, J. A., Clanton, C., Howard, A. W., et al. 2011b, ApJS, 197, 26
Johnson, J. A., Fischer, D. A., Marcy, G. W., et al. 2007, ApJ, 665, 785
Johnson, J. A., Howard, A. W., Bowler, B. P., et al. 2010a, PASP, 122, 701
Johnson, J. A., Marcy, G. W., Fischer, D. A., et al. 2008, ApJ, 675, 784
Johnson, J. A., Morton, T. D., & Wright, J. T. 2013, ApJ, 763, 53
Johnson, J. A., Payne, M., Howard, A. W., et al. 2011a, AJ, 141, 16
Kretke, K. A., Lin, D. N. C., Garaud, P., & Turner, N. J. 2009, ApJ, 690, 407
Kunitomo, M., Ikoma, M., Sato, B., Katsuta, Y., & Ida, S. 2011, ApJ, 737, 66
Kudritzki, R. P., & Reimers, D. 1978, A&A, 70, 227
Laughlin, G. 2000, ApJ, 545, 1064
Lee, B.-C., Han, I., & Park, M.-G. 2013, A&A, 549, A2
Lee, B.-C., Mkrtichian, D. E., Han, I., Kim, K.-M., & Park, M.-G. 2011, A&A, 529, A134
Lin, D. N. C., Bodenheimer, P., & Richardson, D. C. 1996, Nature, 380, 606
Liu, Y.-J., Sato, B., Zhao, G., & Ando, H. 2009, Research in Astronomy and Astrophysics, 9, 1
Liu, Y.-J., Sato, B., Zhao, G., et al. 2008, ApJ, 672, 553
Lloyd, J. P. 2011, ApJ, 739, L49
Mardling, R. A. 2007, MNRAS, 382, 1768
Massarotti, A., Latham, D. W., Stefanik, R. P., & Fogel, J. 2008, AJ, 135, 209
Matsumura, S., Peale, S. J., & Rasio, F. A. 2010, ApJ, 725, 1995
Mazeh, T. 2008, in EAS Pub. Ser. 29, Tidal Effects in Stars, Planets, & Disks, ed. M.-J. Goupil & J.-P. Zahn (Les Ulis: EDP), 1
Ochsenbein, F., Bauer, P., & Marcout, J. 2000, A&AS, 143, 23
Omiya, M., Han, I., Izumioura, H., et al. 2012, PASJ, 64, 34
Perryman, M. A. C., & ESA 1997, in ESA Special Pub. 1200, The HIPPARCOS and TYCHO Catalogues (Noordwijk: ESA)
Rasio, F. A., Tout, C. A., Lubow, S. H., & Livio, M. 1996, ApJ, 470, 1187
Robinson, F. J., Demarque, P., Li, L. H., et al. 2004, MNRAS, 347, 1208
Robinson, S. E., Laughlin, G., Vogt, S. S., et al. 2007, ApJ, 670, 1391
Sackmann, I.-J., Boothroyd, A. I., & Kraemer, K. E. 1993, ApJ, 418, 457
Santos, N. C., Israelian, G., & Mayor, M. 2004, A&A, 415, 1153
Sato, B., Ando, H., Kambe, E., et al. 2003, ApJ, 597, L157
Sato, B., Izumiura, H., Toyota, E., et al. 2007, ApJ, 661, 527
Sato, B., Omiya, M., Liu, Y., et al. 2010, PASJ, 62, 1063
Sato, B., Toyota, E., Omiya, M., et al. 2008, PASJ, 60, 1317
Setiawan, J., Rodmann, J., da Silva, L., et al. 2005, A&A, 437, L31
Sneden, C. A. 1973, PhD thesis, Univ. Texas, Austin
Spitzer, L., Jr., & Schwarzschild, M. 1951, ApJ, 114, 385
Torres, G., Andersen, J., & Giménez, A. 2010, A&A Rev., 18, 67
Torres, G., Fischer, D. A., Sozzetti, A., et al. 2012, ApJ, 757, 161
van Leeuwen, F. 2007, in Astrophys. and Space Sci. Lib. 350, Hipparcos, The New Reduction of the Raw Data (Berlin Heidelberg: Springer-Verlag)
Valenti, J. A., & Fischer, D. A. 2005, ApJS, 159, 141
Valenti, J. A., & Piskunov, N. 1996, A&AS, 118, 595
Villaver, E., & Livio, M. 2009, ApJ, 705, L81
Wittenmyer, R. A., Endl, M., Wang, L., et al. 2011, ApJ, 743, 184
Wright, J. T., Fakhouri, O., Marcy, G. W., et al. 2011, PASP, 123, 412